1258 – 1261; c) D. A. McMorran, P. J. Steel, *Angew. Chem.* **1998**, *110*, 3495 – 3497; *Angew. Chem. Int. Ed.* **1998**, *37*, 3295 – 3297; d) P. R. Ashton, S. J. Cantrill, J. A. Preece, J. F. Stoddart, Z. H. Wang, A. J. P. White, D. J. Williams, *Org. Lett*. **1999**, *1*, 1917 – 1920.

[4] M. Gellert, M. N. Lipsett, D. R. Davies, *Proc. Natl. Acad. Sci. USA* **1962**, *48*, 2013.

[5] W. Guschlbauer, J. F. Chantot, D. J. Thiele, *J. Biomol. Struct. Dyn.* **1990**, *8*, 491 – 511.

[6] T. J. Pinnavaia, C. L. Marshall, C. M. Mettler, E. D. Becker, *J. Am. Chem. Soc.* **1978**, *100*, 3625 – 3627.

[7] M. Borzo, C. Detellier, P. Laszlo, A. Paris, *J. Am. Chem. Soc.* **1980**, *102*, 1124 – 1134.

[8] E. Bouhoutsos-Brown, C. L. Marshall, T. J. Pinnavaia, *J. Am. Chem. Soc.* **1982**, *104*, 6576 – 6584.

[9] a) J. T. Davis, S. Tirumala, J. R. Jenssen, E. Radler, D. Fabris, *J. Org. Chem*. **1995**, *60*, 4167 – 4176; b) M. Cai, A. L. Marlow, J. C. Fettinger, D. Fabris, T. J. Haverlock, B. A. Moyer, J. T. Davis, *Angew. Chem.* **2000**, *112*, 1339 – 1341; *Angew. Chem. Int. Ed.* **2000**, *39*, 1283 – 1285; c) X. Shi, J. C. Fettinger, M. Cai, J. T. Davis, *Angew. Chem.* **2000**, *112*, 3254 – 3257; *Angew. Chem. Int. Ed.* **2000**, *39*, 3124 – 3127; d) F. W. Kotch, J. C. Fettinger, J. T. Davis, *Org. Lett.* **2000**, *2*, 3277 – 3280; e) X. Shi, J. C. Fettinger, J. T. Davis, *J. Am. Chem. Soc*. **2001**, in press.

[10] G. Gottarelli, S. Masiero, G. P. Spada, *J. Chem. Soc. Chem. Commun*. **1995**, 2555 – 2557.

[11] a) A. L. Marlow, E. Mezzina, G. P. Spada, S. Masiero, J. T. Davis, G. Gottarelli, *J. Org. Chem*. **1999**, *64*, 5116 – 5123; b) S. L. Forman, J. C. Fettinger, S. Pieraccini, G. Gottarelli, J. T. Davis, *J. Am. Chem. Soc.* **2000**, *122*, 4060 – 4067.

[12] V. Andrisano, G. Gottarelli, S. Masiero, E. H. Heijne, S. Pieraccini, G. P. Spada, *Angew. Chem.* **1999**, *111*, 2543 – 2544; *Angew. Chem. Int. Ed*. **1999**, *38*, 2386 – 2388.

[13] A cation is not always required for G-quartet formation: J. L. Sessler, M. Sathiosatham, K. Doerr, V. Lynch, K. A. Abboud, *Angew. Chem.* **2000**, *112*, 1356 – 1359; *Angew. Chem. Int. Ed.* **2000**, *39*, 1300 – 1303.

[14] The G-quartet's diastereotopic faces are defined so that the "head" has a clockwise rotation of the N–H $\cdots$ O=C hydrogen bonds. As depicted in Scheme 1, the four D-ribose sugars are located on the G-quartet's "tail".

[15] Crystal data for $(G\mathbf{1})_{16}\cdot 2Sr^{2+}\cdot 4Pic^{-}\cdot (H_2O)_{23.25}\cdot (CH_3CN)_{3.5}$: $C_{335}H_{561}Sr_2N_{95.5}O_{131.25}Si_{16}$; $M_r = 8651.47$, crystal dimensions $0.636\times 0.455\times 0.127$ mm^3, tetragonal, space group $I4$, $a = 30.5043$, $b = 30.5043$, $c = 25.802(3)$ Å, $V = 24{,}009(3)$ Å^3, $Z = 2$, $D_x = 1.197$ mg m^{-3}, $\mu Mo_{K\alpha} = 0.347$ mm^{-1}. Data were collected on a Bruker SMART 1000 CCD diffractometer at 193(2) K. Structure determination was done by direct methods using the program XS.[20] Refinement, using the XL program,[21] was done to convergence on F^2 with $R(F) = 11.12\,\%$ and $wR(F^2) = 23.43\,\%$ for all 15685 independent reflections [$R(F) = 8.84\,\%$, $wR(F^2) = 22.09\,\%$ for those 12150 data with $F_o > 4\sigma(F_o)$]. Crystallographic data (excluding structure factors) for the structure reported in this paper have been deposited with the Cambridge Crystallographic Data Centre as supplementary publication no. CCDC-160231. Copies of the data can be obtained free of charge on application to CCDC, 12 Union Road, Cambridge CB2 1EZ, UK (fax: (+44) 1223-336-033; e-mail: deposit@ccdc.cam.ac.uk).

[16] G. Gottarelli, S. Masiero, G. P. Spada, *Enantiomer* **1998**, *3*, 429 – 438.

[17] [2.2.2]-cryptand binds Ba^{2+} strongly ($K_A > 10^{11}$ M^{-1}): J.-M. Lehn, J. P. Sauvage, *J. Am. Chem. Soc.* **1975**, *97*, 6700 – 6707.

[18] Monitoring picrate coordination by NMR: a) V. Böhmer, A. Dalla Cort, L. Mandolini, *J. Org. Chem.* **2001**, *66*, 1900 – 1902; b) G. G. Talanova, N. S. A. Elkarim, V. S. Talanov, R. E. Hanes, H.-S. Hwang, R. A. Bartsch, R. D. Rogers, *J. Am. Chem. Soc.* **1999**, *121*, 11281 – 11290.

[19] Fortunately, $(G\mathbf{1})_{16}\cdot 2Sr^{2+}\cdot 4Pic^{-}$, $(G\mathbf{1})_{16}\cdot 2Ba^{2+}\cdot 4Pic^{-}$, and $(G\mathbf{1})_8\cdot Ba^{2+}\cdot (G\mathbf{1})_8\cdot Sr^{2+}\cdot 4Pic^{-}$ have similar stabilities so that a statistical distribution of complexes was obtained.

[20] G. M. Sheldrick, *Acta Crystallogr. Sect. A* **1990**, *46*, 467 – 473.

[21] G. M. Sheldrick, Shelxl-93, Program for the Refinement of Crystal Structures, **1993**, University of Göttingen, Germany.

Nickel(II) Phosphate VSB-5: A Magnetic Nanoporous Hydrogenation Catalyst with 24-Ring Tunnels**

Nathalie Guillou, Qiuming Gao, Paul M. Forster, Jong-San Chang, Marc Noguès, Sang-Eon Park,* Gérard Férey,* and Anthony K. Cheetham*

Aluminosilicate zeolites and related nanoporous materials are used widely in the domains of separation, ion-exchange, and shape-selective catalysis.[1–3] The majority of catalytic processes that use zeolites involve acid-catalyzed reactions, for example hydrocarbon isomerization, cracking, alkylation, and dehydration,[1, 3] though recently there has been a surge in interest in partial oxidation reactions based upon titanosilicate materials and transition metal substituted aluminophosphates.[4] It would be of great interest to create nanoporous materials that catalyze other types of reactions, such as shape-selective hydrogenations, but it has not so far proved possible to achieve this in a zeolite catalyst without introduction of extra-framework Ni and noble metal clusters. The underlying challenge here is to design a nanoporous system based on, say, nickel, that is both functional and thermally stable with respect to chemical or structural degradation.[5, 6] We recently showed that the open-framework nickel(II) phosphate, VSB-1 (Versailles – Santa Barbara-1), is sufficiently stable to be rendered nanoporous and exhibits typical zeolitic properties.[7] Furthermore, this large-pore material has interesting catalytic properties suitable for reactions that require only weak acidity.[8] Herein, we describe a second nanoporous nickel phosphate, VSB-5, which exhibits redox properties that

[*] Prof. G. Férey, Prof. A. K. Cheetham, Dr. N. Guillou, Dr. Q. Gao
Dr. M. Noguès
Institut Lavoisier, UMR CNRS C 8637
Université de Versailles Saint-Quentin-en-Yvelines
45 avenue des Etats-Unis, 78035 Versailles Cedex (France)
Fax: (+33) 1-39-25-43-58
E-mail: ferey@chimie.uvsq.fr
cheetham@mrl.ucsb.edu

Prof. A. K. Cheetham, Dr. Q. Gao, P. M. Forster, Dr. J.-S. Chang
Materials Research Laboratory
University of California
Santa Barbara, CA 93106 (USA)
Fax: (+1) 805-893-8797

Dr. S.-E. Park, Dr. J.-S. Chang
Catalysis Center for Molecular Engineering
Korea Research Institute of Chemical Technology (KRICT)
P. O. Box 107, Yusung, Taejon 305-606 (Korea)
Fax: (+82) 42-860-7676
E-mail: separk@pado.krict.re.kr

[**] A.K.C. thanks the Fondation de l'Ecole Normale Supérieure and the Région de l'Ile de France for a Chaire Internationale de Recherche, Blaise Pascal. We also thank the CNRS for financial support and for providing a Poste Rouge for Q.G. and a PICS to the two groups for cooperation. The authors are indebted to D. S. Kim for his support with pore size analysis. We thank the Korean Ministry of Science and Technology (Key Research Program, KK-0005-F0) for supporting this work, and the Korea Science and Engineering Foundation (KOSEF) Fellowship for J.S.C. is gratefully acknowledged. J.S.C. was partially supported by the U.S. Department of Energy under grant DE-FG03-96ER14672. P.M.F. was supported by the National Science Foundation under the MRSEC Program (NSF-DMR-96-32716).

enable it to catalyze partial hydrogenation reactions with high selectivity.

$Ni_{20}[(OH)_{12}(H_2O)_6][(HPO_4)_8(PO_4)_4]\cdot 12H_2O$ VSB-5

VSB-5 can be synthesized between pH 7.3 and 11.0, and over a wide range of Ni/P ratios and concentrations, with little apparent change in the product. Although VSB-5 has not been prepared without an amine present, the particular amine does not seem to be important. For example, we have used a range of diamines from 1,2-ethylenediamine through to 1,8-octanediamine. In a typical synthesis, $NiCl_2\cdot 6H_2O$ (6.0 g; Aldrich) was dissolved in H_2O (60 mL), followed by the addition of H_3PO_4 (6.2 g, 85 %, Fisher) and 1,3-diaminopropane (9.8 g, Aldrich). A green precipitate formed during the addition of the amine, but dissolved with stirring. The final solution was deep purple with a pH of 9.0. After heating in a 120 mL Teflon-lined Parr autoclave at 180 °C for five days, phase-pure VSB-5 was present as a brown solution at pH 10.1. Elemental analysis gave the following results: Ni 40.66 wt %, and P 12.84 wt %. IR spectroscopy revealed that neither amine nor ammonium were introduced into the structure.

X-ray thermodiffractometry[9] shows that the structure of the parent phase is clearly sustained up to about 723 K (Figure 1). It then collapses to form an amorphous phase and recrystallizes to yield condensed $Ni_3(PO_4)_2$ at higher temperatures. Thermogravimetric analysis (TGA)[10] (see insert in Figure 1) of the VSB-5 revealed distinct weight losses of 7.3 (up to 130 °C), 5.7 (200 to 400 °C), 5.7 (450 °C), and 1.1 % (500 to 850 °C). Taken together with the chemical analysis and the structure (see below), these results suggest the chemical composition given above.

Brunauer–Emmet–Teller (BET)[11] surface area and pore structure analysis gives a typical Type-1 isotherm and a surface area of 500(10) m^2g^{-1}. The surface area per gram is comparable to that of a large-pore zeolite, considering that VSB-5 ($\sim$2.6 $g cm^{-3}$) is approximately two times more dense than a typical zeolite. To our knowledge, this surface area is the highest value reported to date for open-framework metal phosphate materials. The pore size distribution, which was monodisperse, gave a pore radius of about 6.4 Å by using the method of Horvath–Kawazoe.

The structure of VSB-5 was solved by ab initio structure solution from laboratory data.[12] Pattern indexing, which was performed by using the computer program DICVOL91,[13] yielded a hexagonal unit cell ($a = 18.209(1)$, $c = 6.3898(7)$ Å; $V = 1834.8(3)$ Å^3). Systematic absences ($0k0$, $k = 2n+1$) were consistent with the space groups $P6_3$ and $P6_3/m$. Structure solution from the X-ray powder diffraction data was performed with the EXPO package, integrating EXTRA,[14] a full pattern decomposition program, and SIR97.[15] The centrosymmetric space group $P6_3/m$ was chosen to solve the structure, and the atomic coordinates obtained by direct methods were used as the starting model in the Rietveld refinement using FULLPROF.[16] Figure 2 shows the final fit obtained between calculated and observed patterns. It corresponds to satisfactory crystal model indicators ($R_B = 0.068$ and $R_F = 0.054$) and profile factors ($R_P = 0.100$ and $R_{wP} = 0.129$).[17]

The view of the structure given in Figure 3 shows that VSB-5 presents a one-dimensional system of pores running in the [001] direction. These tunnels are delineated by 24 NiO_6 octahedra, which are connected by sharing faces, edges, and corners. The pore diameter, based on the distance across the pore of the activated solid (10.2 Å), is in reasonable agreement with the value from the porosimetry data (12.8 Å) when the radii of coordinated oxygen atoms are considered.

Magnetic susceptibility and magnetization measurements[18] reveal antiferromagnetic ordering at 14 K with a Curie–Weiss θ value of -49.5 K. There is evidence of a second magnetic transition at about 6 K, which possibly involves spin canting. The low value of T_N in relation to θ is similar to that found in VSB-1,[7] suggesting that the structure may be magnetically frustrated.

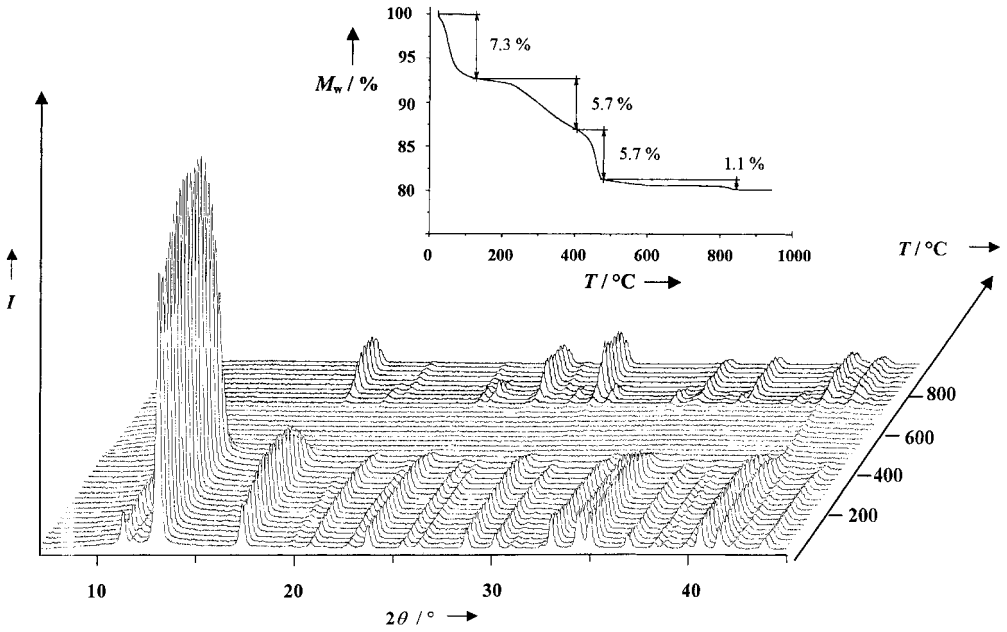

Figure 1. Thermal evolution of the diffractograms during the heating of VSB-5 in air (the line at 41.7° (2θ) in the amorphous zone corresponds to pollution of Pt strip). The TGA curve under oxygen is shown as an insert. I = intensity in arbitrary units.

In view of the possible accessibility of framework Ni atoms for catalytic reactions, we explored the hydrogenation activity of VSB-5.[19] The reduction of 1,3-butadiene to butenes, which requires mild hydrogenation ability, was chosen for this purpose. Selective hydrogenation of 1,3-butadiene to 1-butene in the C4 fraction plays an important role for the production of high-purity alkene streams on an industrial scale.[20] VSB-1 and $Ni_3(PO_4)_2$ were run for comparison. The results show the remarkable perform-

  1433-7851/01/4015-2832 $ 17.50+.50/0

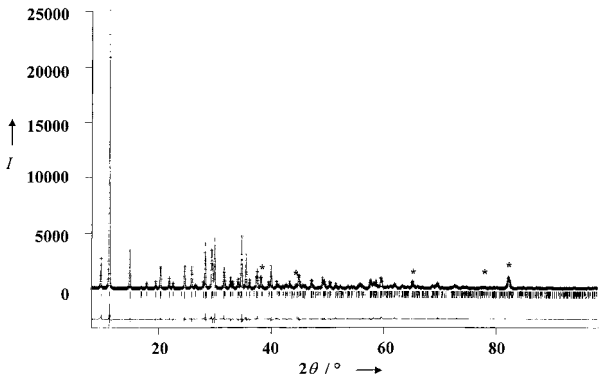

Figure 2. Final Rietveld plot for VSB-5. Observed (crosses) and calculated (line) powder X-ray data, the lower line is the difference curve. Asterisks (*) indicate spurious lines of the sample holder. I = X-ray intensity in arbitrary units.

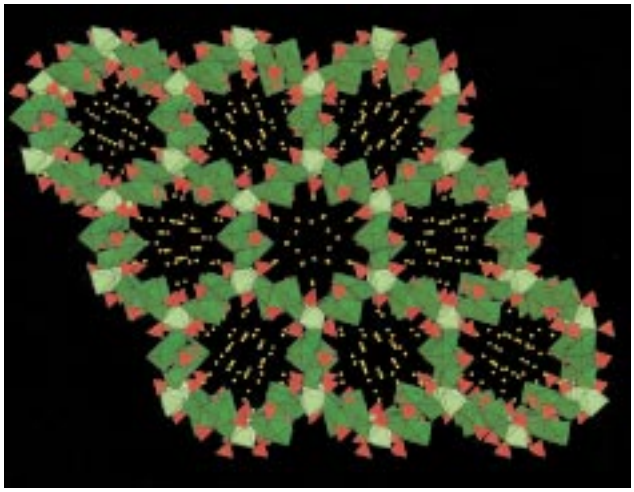

Figure 3. A view of the structure of VSB-5 down [001]. NiO_6 octahedra are shown in light green (disordered Ni3) and dark green (Ni1 and Ni2) and PO_4 tetrahedra are shown in red.

ance of VSB-5 in this reaction (Table 1). VSB-1, by comparison, was only mildly active, while condensed $Ni_3(PO_4)_2$ shows strong hydrogenation activity leading to a high selectivity for butane. The different selectivities of VSB-5 and condensed $Ni_3(PO_4)_2$ for butenes (see Table 1 for the main butenes formed) suggest the availability of framework Ni atoms in the nanoporous structure for selective hydrogenation. Further studies on shape-selective hydrogenation of di-olefins with different molecular dimensions are currently underway.

In the light of the basic synthetic conditions and the abundant hydroxide present in the framework, we investigated whether VSB-5 is capable of supporting base-catalyzed reactions. Using the decomposition of 2-methyl-3-butyn-2-ol (MBOH) as a test reaction,[22] we also examined the acid, base, and even amphoteric properties of VSB-5.[21] The conversion of MBOH gives acetone and acetylene over base sites, or 3-methyl-3-buten-1-yne (Mbyne) with 3-methyl-2-buten-1-al over acid sites. Table 2 shows the catalytic results for the conversion of MBOH over VSB-5 and VSB-1. To our surprise, VSB-5 exhibits very high MBOH conversion (99% at 573 K) as well as high selectivity (>99%) for the formation of acetone and acetylene, unambiguously confirming its base character. In contrast, VSB-1 gives only poor conversion (10%) of MBOH and a mixture of several products at 573 K, indicating that it possesses only poor acidity and basicity.

Table 2. Catalytic conversion of 2-methyl-3-butyn-2-ol over VSB-1 and VSB-5 materials.[a]

Catalyst	S_{BET} [$m^2 g^{-1}$]	T [°C]	MBOH conversion[b] [%]	Selectivity [%] acetone	acetylene	Mbyne[c]
VSB-1	183	250	2.7	38.1	38.9	23.0
		300	10.0	37.9	39.8	22.3
VSB-5	500	250	22.6	49.1	49.0	1.9
		300	99.0	50.2	49.0	0.8

[a] Reaction conditions: p(MBOH) = 2 kPa, W/F = 125 g h mol^{-1}, time on stream = 10 min. [b] MBOH: 2-methyl-3-butyn-2-ol. [c] Mbyne: 3-methyl-3-buten-1-yne.

In summary, VSB-5, a nanoporous nickel phosphate, has been synthesized by hydrothermal methods. This new material is found to have four important properties: nanoporosity, good thermal stability, antiferromagnetic ordering, and hydrogenation and basic catalytic character. The basic character presumably stems from the presence of OH anions in the framework. The efficacy of VSB-5 for partial hydrogenation reactions suggests the availability of active sites associated with framework Ni atoms.

Received: February 26, 2001 [Z16683]

[1] A. Corma, *Chem. Rev.* **1997**, *97*, 2373–2419.
[2] M. E. Davis, *Chem. Eur. J.* **1997**, *3*, 1745–1750.
[3] a) J. M. Thomas, *Sci. Am.* **1992**, *266*, 112–118; b) J. M. Thomas, *Angew. Chem.* **1994**, *106*, 963–989; *Angew. Chem. Int. Ed. Engl.* **1994**, *33*, 913–937.
[4] a) T. Taramasso, G. Perego, B. Notari (Eniriceche), US Patent US-A 4410501, **1983**; b) R. J. Saxton, *Top. Catal.* **1999**, *9*, 43–57; c) B. Notari, *Adv. Catal.* **1996**, *41*, 253–334; d) R. Raja, G. Sankar, J. M. Thomas, *Angew. Chem.* **2000**, *112*, 2403–2406; *Angew. Chem. Int. Ed.* **2000**, *39*, 2313–2316; e) J. Chen, R. H. Jones, S Natarajan, M. B. Hursthouse,

Table 1. Selective hydrogenation of 1,3-butadiene (BD) over VSB-1 and VSB-5.[a]

Catalyst	H Act.[d] [h]	T [°C]	BD conversion [%]	S_{butene}[e] [%]	Selectivity [%] *n*-butane	1-butene	*trans*-2-butene	*cis*-2-butene
VSB-1[b]	16	200	1.0	99.9	0.1	34.0	36.7	29.2
VSB-5[b]	4	200	10.3	97.9	2.1	48.4	30.5	19.0
VSB-5[b]	16	200	68.4	97.6	2.4	52.4	28.5	16.7
VSB-5[b]	24	100	81.1	95.8	4.2	50.9	32.0	12.9
VSB-5[c]	16	100	99.6	21.4	78.6	14.0	1.3	6.1
$Ni_3(PO_4)_2$	4	100	99.5	47.7	52.3	27.4	7.3	13.0

[a] Reaction conditions: p(BD) = 10.1 kPa, W/F = 0.3 g s mL^{-1}, H_2/BD = 3, time on stream = 2 h. [b] Calcination at 350 °C for 4 h. [c] Calcination at 550 °C for 4 h. [d] Activation time under 5% H_2 in He at 350 °C. [e] Selectivity to give butene products.

  1433-7851/01/4015-2833 $ 17.50+.50/0

J. M. Thomas, *Angew. Chem.* **1994**, *106*, 667–668; *Angew. Chem. Int. Ed. Engl.* **1994**, *33*, 639–641.
[5] M. A. Drezdzon, *Inorg. Chem.* **1988**, *27*, 4628–4632.
[6] A. K. Cheetham, G. Férey, T. Loiseau, *Angew. Chem.* **1999**, *111*, 3466–3492; *Angew. Chem. Int. Ed.* **1999**, *38*, 3268–3292.
[7] N. Guillou, Q. Gao, M. Nogues, R. E. Morris, M. Hervieu, G. Férey, A. K. Cheetham, *C. R. Acad. Sci. Paris* **1999**, *2*, 387–392.
[8] J.-S. Chang, S.-E. Park, Q. Gao, G. Férey, A. K. Cheetham, *Chem. Commun.* **2001**, *9*, 859–860.
[9] Thermodiffractometry was performed under air in an Anton Paar HTK16 high-temperature device of a Siemens D5000 X-ray powder diffractometer ($\theta-\theta$ mode; $Co_{K\alpha}$ radiation $\lambda = 1.7903$ Å), equipped with a M Braun linear position sensitive detector (PSD). Patterns were scanned with a resolution of 0.0147° and a divergence slit of 0.1° over an angular range of 5–50° (2θ), at 25 °C intervals up to 1000 °C; rate of increase of temperature: 0.1 °C s^{-1}; see Figure 1.
[10] TGA data were obtained on a TGA 2050 thermogravimetric analyser thermobalance using a sample synthesized by using 1,3-diaminopropane.
[11] BET analysis was performed by using a Micromeritics ASAP2400 porosimeter on a sample activated at 350 °C for four days.
[12] The X-ray powder diffraction data for VSB-5 were collected on a Siemens D5000 diffractometer by using $Cu_{K\alpha}$ radiation ($\lambda = 1.5418$ Å). To avoid preferred orientation effects, the synthesis was carried out under stirring conditions, keeping the same experimental conditions with the same molar ratio and filling rate. The resulting powder was then loaded in the sample holder. The powder diffraction pattern was scanned over an angular range of 4–120° (2θ). The counting times were 27 s per step to 59.98° (2θ) and 54 s per step from 60.00° (2θ) to the end of the scan (to improve the counting statistics of the high-angle region). The full pattern was then scaled to the lower counting time. An accurate determination of the peak positions and relative intensities was carried out by using the software package DIFFRACT-AT.
[13] A. Boultif, D. Louër, *J. Appl. Crystallogr.* **1991**, *24*, 987–993.
[14] A. Altomare, M. C. Burla, G. Cascarano, C. Giacovazzo, A. Guagliardi, A. G. G. Moliterni, G. Polidori, *J. Appl. Crystallogr.* **1995**, *28*, 842–846.
[15] A. Altomare, M. C. Burla, M. Camalli, G. L. Cascarano, C. Giacovazzo, A. Guargliardi, A. G. G. Moliterni, G. Polidori, R. Spagna. *J. Appl. Crystallogr.* **1999**, *32*, 115–119.
[16] J. Rodriguez-Carvajal, *Collected Abstracts of Powder Diffraction Meeting* (Toulouse, France) **1990**, p. 127.
[17] Further details on the crystal structure investigation may be obtained from the Fachinformationszentrum Karlsruhe, 76344 Eggenstein-Leopoldshafen, Germany (fax: (+49) 7247-808-666; e-mail: crysdata@fiz-karlsruhe.de), on quoting the depository number CSD-411917.
[18] Magnetization measurements were performed in the temperature range 4–295 K at 5 kG and 100 G on a Quantum Design Squid magnetometer (MPMS-5).
[19] The selective hydrogenation of 1,3-butadiene to butenes was carried out in a continuous fixed-bed reactor made of quartz at atmospheric pressure. Before catalytic measurement, the catalyst was reduced with 5% hydrogen in helium at 350 °C for 4–24 h. The reaction was carried out while introducing mixture of 1,3-butadiene (99.0%) and pure hydrogen under helium. The effluent stream from the reactor was analyzed by an on-line gas chromatograph (HP 5890 Series II) fitted with a capillary column (J&W Alumina) and a flame-ionization detector.
[20] H. Arnold, F. Doebert, J. Gaube in *Handbook of Heterogeneous Catalysis*, *Vol. 5* (Eds.: G. Ertl, H. Knoezinger, J. Weitkamp), VCH, Weinheim, **1997**, pp. 2165–2186.
[21] E. Iglesia, D. G. Barton, J. A. Biscardi, M. J. L. Gines, S. L. Soled, *Catal. Today* **1997**, *38*, 339–360.
[22] Decomposition of MBOH (>99%, Aldrich) was carried out in a plug-flow glass reactor with an internal diameter of 10 mm. The MBOH was placed in a vaporizer in which a helium flow was saturated with the alcohol vapor at 298 K and then the MBOH/helium mixture was fed into the reactor. The catalytic activity of VSB-5 was examined after the calcination of the fresh sample at 623 K for 4 h in air. Reaction products were analyzed by an on-line gas chromatograph (Hewlett-Packard model 5890II) fitted with a capillary column (J&W DB-WAX) and a flame-ionization detector.

Spherical Aromaticity of Inorganic Cage Molecules**

Andreas Hirsch,* Zhongfang Chen, and Haijun Jiao

We have shown recently that the icosahedral fullerenes C_{20}, C_{60}, and C_{80} reach maximum spherical aromaticity if their π shells are completely filled.[1] This is nicely demonstrated, for example, by the very pronounced diatropic character of the $2(N+1)^2$ π systems of the C_{20}^{2+} ($N=2$), C_{60}^{10+} ($N=4$), and C_{80}^{8+} ($N=5$) ions with perfect I_h symmetry. Here we extend this treatment of spherical aromaticity to a set of well-known inorganic cage compounds and demonstrate that they are highly aromatic because of the closed-shell nature of both their σ and π systems.

Tetrahedral clusters P_4 and As_4 form metastable solid allotropes, whereas Sb_4 and Bi_4 are high-temperature modifications existing only in liquid or in the gas phase. Tetrahedral N_4 (T_d), being the most stable singlet N_4 isomer,[2] was recently generated in a plasma as the first neutral polynitrogen species.[3] The calculated nucleus-independent chemical shifts (NICS)[4, 5] at the cage centers of these T_d-symmetrical clusters with optimized bond lengths (Figure 1)

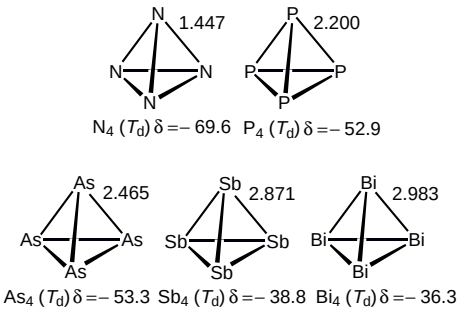

Figure 1. Optimized bond lengths [Å] and NICS values [δ] for E_4 (T_d) clusters (E = N, P, As, Sb, Bi).

are given in Table 1. The highly negative NICS values of all clusters are a result of pronounced diamagnetic ring currents. The pronounced diatropic character of these clusters is not a result of the addition of four individual increments consisting of three-membered rings, but a new quality of the entire cages. This is clearly reflected by the fact that: 1) the NICS and the NICS per valence electron (NICS/e) values in the center of the cages are considerably more negative than those in the

[*] Prof. Dr. A. Hirsch, Dr. Z. Chen, Dr. H. Jiao[+]
Institut für Organische Chemie der Universität Erlangen-Nürnberg
Henkestrasse 42
91054 Erlangen (Germany)
Fax: (+49) 9131-85-26864
E-mail: hirsch@organik.uni-erlangen.de
[+] Laboratoire de Chimie du Solide et Inorganique Moléculaire
UMR 6511 CNRS, Université de Rennes 1, Institut de Chimie de Rennes, 35042 Rennes Cedex (France)
[**] This work was supported by the Alexander von Humboldt Stiftung (Z. Chen), the Centre National de la Recherche Scientifique (H. Jiao), and the Fonds der Chemischen Industrie. We thank Prof. Dr. T. F. Fässler for his helpful discussion and reprints.

  1433-7851/01/4015-2834 $ 17.50+.50/0